Thin–Walled Structures 158 (2021) 107171

Contents lists available at ScienceDirect

Thin-Walled Structures

journal homepage: http://www.elsevier.com/locate/tws

Spline finite strip analysis of thin-walled flexural members subjected to general loading with intermediate restraints

S.S. Ajeesh [a,*], S. Arul Jayachandran [b]

[a] School of Civil Engineering, Vellore Institute of Technology, Vellore, India
[b] Department of Civil Engineering, Indian Institute of Technology, Madras, India

ARTICLE INFO

Keywords:
Spline finite strip method
Thin-walled steel
Mode decomposition
Generalized beam theory
Flexural member

ABSTRACT

The design of cold-formed steel flexural members using the Direct Strength Method (DSM), use signature curves of cross-sections with the assumption of equal end moments and uniform stresses in the longitudinal direction. However, for beams subjected to general transverse loads, the assumption of longitudinal uniform stress is conservative. In calculating elastic critical loads of thin-walled flexural members, to incorporate a non-uniform variation of longitudinal stresses, this paper presents a spline finite strip computational procedure, which can also be used for beams with intermediate restraints. To the authors' knowledge, such a procedure using spline finite strip is presented for the first time in the literature. The present formulation is comprehensive in its generality compared with similar works published. The membrane and shear stresses due to transverse loads on the beam are determined in the local direction of the plate at section knots of the spline strip. These stresses are incorporated in the geometric stiffness matrix, and buckling analysis is performed for calculating the elastic buckling load. Restraint matrices are incorporated in buckling analysis for the decomposition of buckling modes and for calculating mode participation. The proposed formulation is compared with generalized beam theory (GBT) for lipped channel cross-section with variation in span, general loading, and intermediate restraints. This method is demonstrated to be good for calculating elastic buckling stresses for the practical design of thin-walled flexural members.

1. Introduction

Cross-sectional and member instabilities such as local, distortional, and global buckling are the main parameters determining the design capacity of thin-walled steel sections. Direct strength method (DSM) design of thin plated steel compression and flexural members considers these instabilities in the form of elastic buckling stress. Elastic buckling strength of the thin-walled steel section is dependent mainly on the geometry of member, and the buckling stresses for global, distortional, and local buckling can be evaluated either by analytical expression or numerical methods. Finite strip method (FSM), which requires less computational effort, has been recommended in DSM for determining global, distortional, and local buckling stress. This method is developed initially for static analysis of thin plates [1] and extended to generate the signature curve of thin-walled flexural members [2]. The signature curve in FSM has been developed using the assumption of uniform compressive or flexural stresses in the longitudinal direction of the member with simply supported boundary condition for columns and beams.

Practical thin-walled flexural members can have variation in bending stress along the longitudinal direction in the presence of different transverse loads/moments, and these members may also have different supports and intermediate restraint conditions. Since a continuous trigonometric function is used for longitudinal interpolation, analysis with discrete intermediate constraints and non-uniform stresses in the longitudinal direction of the plate is difficult in traditional FSM. However, research on the application of general loading conditions in the context of traditional FSM is presented in Ref. [3]. The strategy adopted is to divide the longitudinal strip into different cells, and numerical integration is performed separately on each cell for corresponding stresses. In a recent study [4], multiple series terms are incorporated for longitudinal interpolation in the context of FSM for buckling analysis of thin-walled beams subjected to localized loading. A study has been reported on the influence of uniformly distributed load on local and distortional buckling capacity of cold-formed steel members based on FSM [5]. Also, buckling analysis has been presented for localized

* Corresponding author.
E-mail address: ajeeshss.tkm@gmail.com (S.S. Ajeesh).

https://doi.org/10.1016/j.tws.2020.107171
Received 19 April 2020; Received in revised form 24 August 2020; Accepted 22 September 2020
Available online 15 October 2020

loading conditions in flexural members using FSM by considering pre-buckling membrane and flexural stresses [6]. Generalized beam theory (GBT) is ideally suited for buckling analysis and mode extraction of thin-walled sections, and this technique is used for first and second-order analysis of thin-walled steel members [7]. The non-standard support conditions and different transverse loading conditions have been incorporated in classical GBT [8].

Spline finite strip method (SFSM) is introduced for static analysis of thin-walled members by considering different loading, and support conditions [9] and this formulation is further modified for buckling analysis by introducing geometric stiffness matrix, which incorporates membrane stresses in the form of transverse and longitudinal compression and also shear stress acting along the edges of plate strip [10]. Other developments in the incorporation of SFSM in thin-walled steel members include nonlinear analysis for calculating post-buckling response [11–13], iso-parametric spline finite strip formulation for elastic buckling analysis of perforated thin-walled members [14] and its extension to nonlinear analysis by considering the material and geometric nonlinearity [15–17].

The buckling stresses calculated for different member lengths using SFSM is the interactive solution, where buckling modes like local, distortional, global and other (shear/transverse extension) modes interact each other, and the stress calculated using SFSM may not be suitable as design input for practical member lengths using DSM. A technique for extracting pure buckling modes in the context of FSM has been proposed [18–20] by developing restraint matrices corresponding to global, distortional, and local buckling modes calculated based on GBT fundamental assumptions. The proposed technique termed as constrained finite strip method (cFSM) has also been developed for thin-walled cross-sections with closed and branched shapes [21], classification of deformation modes into different subfields [22,23], members with different boundary conditions [24] and calculation of percentage participation of different modes in buckling analysis using FSM [25]. Similarly, studies are reported on the integration of GBT principles in finite element formulation for mode decomposition [26,27], mode identification for elastic buckling analysis [28–30], and nonlinear analysis [31]. Recent studies in this area include the development of constrained shell finite element model [32], development of constrained finite element technique for thin-walled steel members [33,34], and its extension to perforated sections [35]. A mode decomposition strategy has also been proposed in the context of FSM using energy principles for the decomposition of buckling modes [36,37].

Considering the advantages of SFSM, constrained spline finite strip method (cSFSM) and identification of buckling modes in generalized buckling analysis [38,39] have been proposed by integrating GBT principles in SFSM. The validation problems in the study are presented mainly for cold-formed steel members under uniform flexural and compressive stress in longitudinal direction. Constrained spline finite strip analysis that decomposes global and distortional modes for members with branched open cross-sections and closed cross-sections has also been proposed [40].

Of course, several studies in the direction of the theme of the paper have been published. The objective of this paper is the development of cSFSM for thin-walled flexural members subjected to variation in flexural stress along the longitudinal direction of the member under different transverse loading conditions. Existing studies on cSFSM consider uniform flexural stress distribution along member length for decomposition and identification of buckling modes. The present study is more comprehensive in its generality by incorporating longitudinal discontinuities in terms of stresses and intermediate restraints in the context of cSFSM compared to existing studies that are available in the literature. The incorporation of variation in flexural stress along the length of member enables the utilization of additional elastic buckling strengths in terms of different buckling modes in DSM design for members subjected to transverse loads. In this study, uncoupled buckling loads for global, distortional, and local buckling are calculated for members subjected to different transverse loadings, and the percentage contribution of each buckling mode in generalized buckling analysis is determined. Also, the flexibility of the proposed cSFSM in incorporating discrete intermediate restraints with different end conditions and the enhancement in buckling stresses due to incorporation of flexural stress variation in the longitudinal direction for the analysis of flexural members is demonstrated.

2. A brief on constrained spline finite strip method (cSFSM)

Basic spline finite strip analysis and incorporation of GBT principles for decomposition and identification of individual buckling modes in SFSM are available in various works presented in literature [9,38,39]. However, for completeness, the procedure incorporated in SFSM and cSFSM for buckling analysis are briefly presented. A cold-formed steel member as a result of longitudinal discretization with a global-local coordinate system and stress distribution of a plate strip is provided in Fig. 1. The nodal line in a plate strip corresponds to several section knots with four degrees of freedom (u, v, w, θ) at each knot along the nodal line. The membrane and shear stress acting on the edges of the plate strip is dependent on the type of load acting on the member.

The deformation of the plate strip is classified as flexural (w, θ) and membrane (u, v) displacements based on Kirchhoff's thin plate theory and plane stress condition, respectively. For both flexural and membrane deformation, cubic splines are used for interpolating displacements in the longitudinal direction with different spline amendment schemes for end conditions. In the transverse direction of the plate, flexural displacements are interpolated using cubic Hermitian functions and membrane displacements using the Lagrangian interpolation function.

For buckling analysis, the geometric stiffness matrix is calculated under the assumption of longitudinal (σ_y), transverse (σ_x) and shear (σ_{xy}) stresses acting at the edges of the plate as given in Fig. 1b. The work done by flexural and membrane displacements due to nonlinear strains acting on the plate under membrane and shear edge stresses is calculated for individual plate strip. The Eigenvalue problem for buckling analysis is developed by minimizing the total potential energy in SFSM.

The constraining condition for different buckling modes is imposed by introducing a restraint matrix containing base vectors contributing to a particular mode. Using a transformation technique, the constraints are imposed in the Eigenvalue equation. The percentage contribution of individual base vectors in a particular mode shape in generalized spline finite strip analysis is obtained by representing the displacement function corresponding to a particular mode as a combination of orthonormal base vectors linearly, and approximating the error to be minimum.

3. Incorporation of general loading conditions and intermediate restraints in SFSM

For determining the elastic buckling stresses to be adopted in DSM using FSM for the design of thin-walled flexural members, the assumption of uniform flexural stress in the longitudinal direction and simply supported flexural end conditions are incorporated. The variation of bending stresses along the length of the beam is not considered in FSM. This results in lower bound strength prediction for general loading conditions. Also, in professional practice, cold-formed steel members may have intermediate web/flange restraints. The incorporation of non-uniform flexural stresses in the longitudinal direction and intermediate restraints in SFSM for calculating elastic buckling stresses are explained.

3.1. cSFSM for general loading conditions

For buckling analysis in SFSM, the geometric stiffness matrix ($[K_g]$) corresponding to general loads need to be developed. The edge stresses acting on each plate strip (σ_x, σ_y, σ_{xy}) corresponding to transverse loads

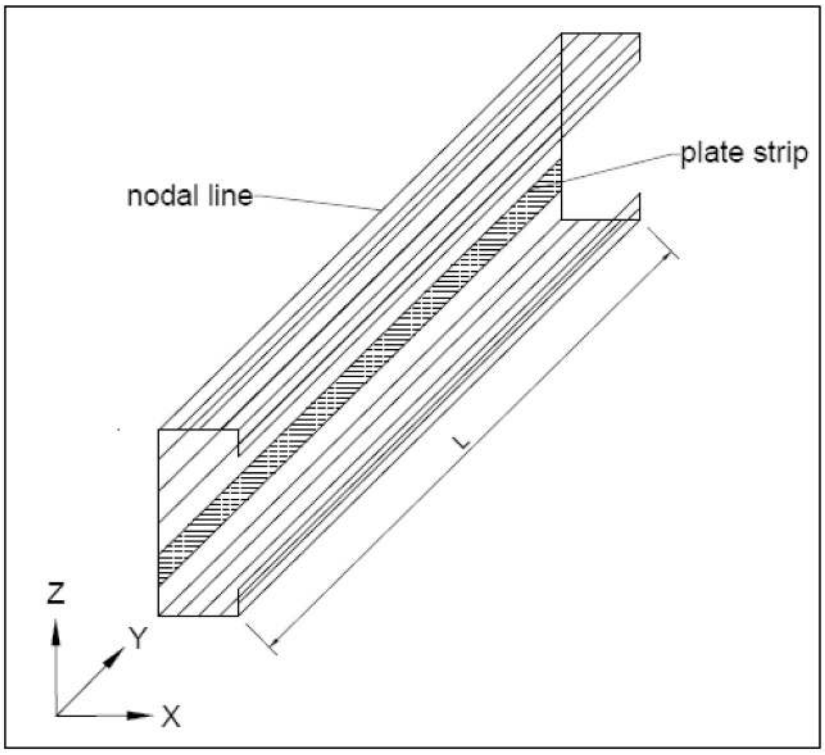

(a) Thin-walled steel member with the global coordinate system

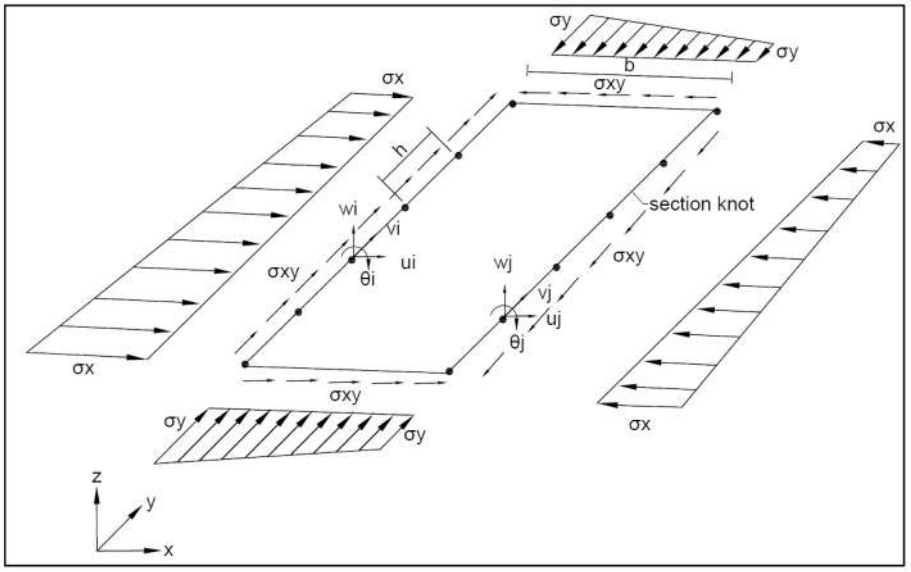

(b) Longitudinal strip with edge stresses in the local coordinate system

Fig. 1. Thin-walled member with the degree of freedom and coordinate system.

applied on the beam is determined from the static analysis of the member, as shown in Eq. (1), where $[K]$ is the elastic global stiffness matrix, $\{\delta\}$ is the global displacement vector and $\{F\}_G$ is the global load vector corresponding to general loads acting on the member.

$$[K]\{\delta\} = \{F\}_G \tag{1}$$

The element displacement vector of each plate strip in the global direction ($\{\delta_{e,G}\}$) considering all the section knots in a plate strip is determined (Eq. (2)) from the global displacement vector ($\{\delta\}$) developed as a result of static analysis of the member. The element displacements are transformed into displacements in the local direction of the plate using coordinate transformation, as shown in Eq. (3), where α is the inclination of the plate strip with respect to reference axis in global X direction. The local displacements corresponding to both nodal lines of a plate strip are assembled to obtain the strip displacement vector in the local direction (Eq. (4))

$$\{\delta_{e,G}\} = \{\ U_i \quad V_i \quad W_i \quad \Theta_i \quad U_j \quad V_j \quad W_j \quad \Theta_j\ \}^T \tag{2}$$

$$\begin{Bmatrix} u_i \\ v_i \\ w_i \\ \theta_i \end{Bmatrix} = \begin{bmatrix} cos\,\alpha & 0 & sin\alpha & 0 \\ 0 & 1 & 0 & 0 \\ -sin\alpha 000 & & cos\alpha & 0 \\ & & 0 & 1 \end{bmatrix} \begin{Bmatrix} U_i \\ V_i \\ W_i \\ \Theta_i \end{Bmatrix} \tag{3}$$

$$\{\delta_{e,L}\} = \{\ u_i \quad v_i \quad w_i \quad \theta_i \quad u_j \quad v_j \quad w_j \quad \theta_j\ \}^T \tag{4}$$

From the local displacement vector of plate strip, longitudinal, transverse, and shear strains are evaluated, as shown in Eq. (5), where N and Φ represents the interpolation functions in the transverse and longitudinal direction, and the superscript ($'$) represents the first derivative. The membrane and shear stresses are evaluated from strains using constitutive relation as depicted in Eqs. (6) and (7). Here E_x, ν_x and E_y, ν_y represents the modulus of elasticity and Poisson's ratio in x and y direction of plate strip and G_{xy} represents rigidity modulus of plate strip.

$$\{\varepsilon\}_m = \begin{Bmatrix} \dfrac{\partial u}{\partial x} \\ \dfrac{\partial v}{\partial y} \\ \dfrac{\partial u}{\partial y} + \dfrac{\partial v}{\partial x} \end{Bmatrix} = \begin{bmatrix} N'_{ui}\Phi_{ui} & 0 & N'_{uj}\Phi_{uj} & 0 \\ 0 & N_{vi}\Phi'_{vi} & 0 & N_{vj}\Phi'_{vj} \\ N_{ui}\Phi'_{ui} & N'_{vi}\Phi_{vi} & N_{uj}\Phi'_{uj} & N'_{vj}\Phi_{vj} \end{bmatrix} \{\delta_{e,L}\} \tag{5}$$

$$\{\sigma\}_m = \begin{Bmatrix} \sigma_x \\ \sigma_y \\ \sigma_{xy} \end{Bmatrix} = \begin{bmatrix} D_x & D_1 & 0 \\ D_1 & D_y & 0 \\ 0 & 0 & D_{xy} \end{bmatrix} \begin{Bmatrix} \dfrac{\partial u}{\partial x} \\ \dfrac{\partial v}{\partial y} \\ \dfrac{\partial u}{\partial y} + \dfrac{\partial v}{\partial x} \end{Bmatrix} \tag{6}$$

$$\begin{Bmatrix} D_x = \dfrac{E_x}{(1-\nu_x\nu_y)} \\ D_1 = \nu_x D_y = \nu_y D_x \\ D_y = \dfrac{E_y}{(1-\nu_x\nu_y)} \\ D_{xy} = G_{xy} \end{Bmatrix} \tag{7}$$

The evaluated stresses corresponding to transverse loading on the beam are incorporated in the geometric stiffness matrix for membrane and flexural deformations as provided in Eqs. (8)–(12). The stress variation between section knots and nodal lines are assumed to be linear in the case of longitudinal, transverse, and shear stresses.

$$[K_g]_b = [K_g]_{b1} + [K_g]_{b2} + [K_g]_{b3} \tag{8}$$

$$[K_g]_{b1} = \int_0^a \int_0^b \frac{\partial[\Phi]_b^T}{\partial y}[N]_b^T[N]_b \frac{\partial[\Phi]_b}{\partial y}\sigma_y t\, dxdy \tag{9}$$

$$[K_g]_{b2} = \int_0^a \int_0^b [\Phi]_b^T \frac{\partial[N]_b^T}{\partial x}\frac{\partial[N]_b}{\partial x}[\Phi]_b \sigma_x t\, dxdy \tag{10}$$

$$[K_g]_{b3} = \int_0^a \int_0^b [\Phi]_b^T \frac{\partial[N]_b^T}{\partial x}[N]_b \frac{\partial[\Phi]_b}{\partial y} 2\sigma_{xy} t\, dxdy \tag{11}$$

$$[K_g]_m = \int_0^a \int_0^b \frac{\partial[\Phi]_m^T}{\partial y}[N]_m^T[N]_m \frac{\partial[\Phi]_m}{\partial y}\sigma_y t\, dxdy \tag{12}$$

The critical buckling load is determined by calculating the Eigenvalues from buckling equation (Eq. (13)) using an updated geometric stiffness matrix from stresses corresponding to applied loading after combining membrane and flexural stiffness matrices. Similarly, mode decomposition and mode identification can be performed using the updated geometric stiffness matrix.

$$([K] - \lambda[K_g])\{\delta\} = 0 \tag{13}$$

To demonstrate the development of membrane strains for general loading conditions in SFSM, the static analysis results of a lipped channel with simply supported ends have been compared with finite element method (FEM) calculated using the FEM package, ABAQUS [41]. The span of the beam is selected as 2000 mm and the beam is subjected to a distributed load of 100 N at the web-flange junction on all the section knots along the longitudinal direction. Longitudinally, the member is divided into 20 sections. The cross-sectional dimensions and loading points are depicted in Fig. 2. The plate thickness is taken as 1 mm and modulus of elasticity and Poisson's ratio for the present study is assumed to be 200000 N/mm^2 and 0.3 respectively.

The static analysis of the flexural member is performed using SFSM and the vertical and lateral displacements at web-compression flange junction along the length of the member is compared with FEM results, as shown in Fig. 3. This simple benchmark problem is shown because the stresses that are used in the geometric stiffness matrices have to be necessarily accurate. It has to be noted that the displacement values are considered at 19 intermediate points along the longitudinal direction of the beam, and close comparison is observed between SFSM and FEM results. The cross-section of the beam has been discretized using six, three, and one intermediate node in the web, flange, and lip, respectively. The mesh size incorporated in FEM is the same as that of SFSM, and the finite element used for analysis in FEM is S8R5, which is a shell element having 8 nodes and 5 degrees of freedom per node.

Since the transverse load is acting away from shear center of the cross-section, the member is subjected to torsion along with bending. This is evident from the displacements plotted in Fig. 3 along the length of the member, which has significant lateral displacement along with vertical displacement. From the displacements of plate strips evaluated in the global direction of the member, the membrane and flexural displacements corresponding to each plate strip in local direction have been evaluated using the transformation of coordinates (Eq. (3)). Displacements in the local direction of the plate are used for calculating the membrane strains in local x and y direction and shear strain (Eq. (5)) acting on the edges of the plate strip. From these strains, the longitudinal, transverse, and shear stresses are calculated using Eq. (6) for application in buckling analysis. The stress values computed using the present formulation agrees well with classical solutions.

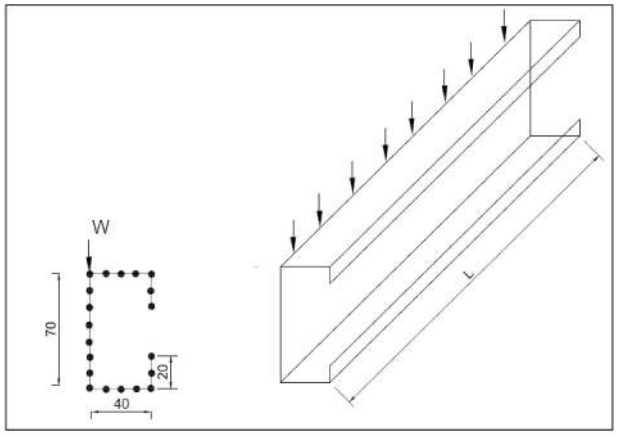

*Dimensions are in millimetres

Fig. 2. Cross section dimensions and loading point.

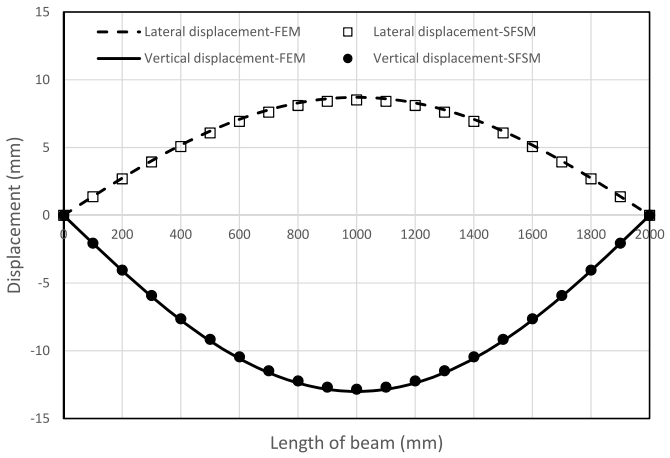

Fig. 3. Comparison of displacement along length of member.

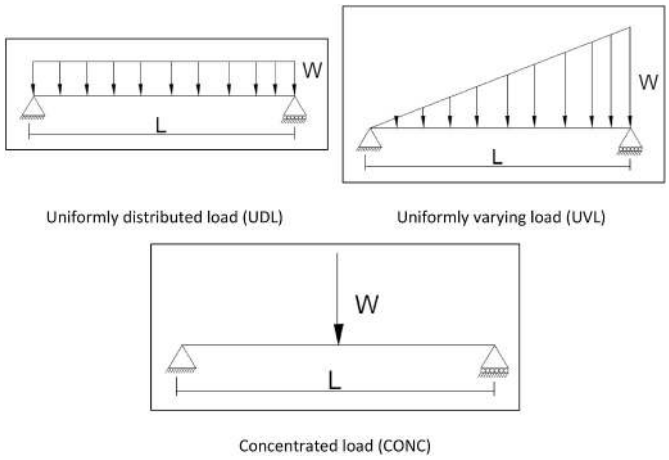

Fig. 4. Loading conditions for comparison of buckling loads.

3.2. Incorporation of intermediate flange/web restraints

The constraints for the degree of freedom on section knots in the spline finite strip model are imposed using the Lagrange multiplier technique in which the algebraic equation corresponding to static analysis is written of the form given in Eq. (14).

$$\begin{bmatrix} [K] & [C_L]^T \\ [C_L] & [0] \end{bmatrix} \begin{Bmatrix} \{\delta\} \\ \{\lambda_L\} \end{Bmatrix} = \begin{Bmatrix} \{F\} \\ \{F_L\} \end{Bmatrix} \tag{14}$$

In the expression, $[C_L]$ represents the matrix corresponding to coefficients in constraint equation, $\{\lambda_L\}$ is the vector of multipliers and $\{F_L\}$ is the load vector corresponding to imposed constraints depending upon the number of constraints considered in the analysis. $[K]$, $\{\delta\}$ and $\{F\}$ represents elastic stiffness matrix, displacement vector, and load vector, respectively. The incorporation of constraints increases the size of the elastic and geometric stiffness matrix depending upon the number of constraints imposed in the analysis. In buckling analysis corresponding to SFSM, the constraints are imposed in Eigenvalue analysis as given in Eq. (15).

$$\begin{bmatrix} [K] & [C_L]^T \\ [C_L] & [0] \end{bmatrix} - \lambda \begin{bmatrix} [K_g] & [C_L]^T \\ [C_L] & [0] \end{bmatrix} = 0 \tag{15}$$

The minimum value of load factor λ corresponds to the critical buckling load, and the participation of individual buckling modes is calculated from the deformation vector obtained in buckling analysis. In this study, the constraints are incorporated in static analysis for determining the membrane stresses of the plate and also for calculating the elastic buckling load in Eigenvalue analysis.

4. Application of general loading conditions and intermediate restraints in SFSM

The demonstration of unconstrained and constrained buckling analysis is performed on the lipped channel cross-section for different lengths of the flexural member. The ends of the beam are assumed as simply supported, and transverse loads are applied at the compression flange-web junction of the beam. The dimensions and discretization of the cross-section is shown in Fig. 2. For all the spans, twenty-one sections knots are assumed along the length of the beam. Fig. 4 represents different loading conditions assumed at the web-compression flange junction of the lipped channel section for unconstrained and constrained buckling analysis.

4.1. Unconstrained buckling analysis

Buckling analysis has been performed for different transverse loads acting along the web-compression flange junction represented in Fig. 4, and the critical buckling load calculated using SFSM is compared with FEM results calculated using ABAQUS and generalized beam theory (GBT) results calculated using GBTUL [42]. Lipped channel member with cross-section details and discretization shown in Fig. 2 has been adopted in SFSM, and the elastic buckling analysis is performed for spans varying from 500 mm to 5000 mm. The discretization of the member is selected based on a mesh sensitivity analysis for four different member lengths, as shown in Fig. 5. It has to be noted that the element size of 10 mm is incorporated in the web, flanges, and lips, as shown in Fig. 2 for the present study. For uniformly distributed load (UDL) and uniformly varying load (UVL), concentrated forces are applied on all the 19 intermediate section knots, excluding the edge supports on web-compression flange junction along the longitudinal direction.

For comparison with SFSM results, elastic buckling analysis using FEM in ABAQUS is performed using a three-dimensional shell finite element model using S8R5 element having 8 nodes within the element and 5 degrees of freedom per node. The material properties and discretization of plate strips are incorporated exactly similar to SFSM. Simply supported boundary conditions are applied at cross-sectional nodes at both ends of the member, and load is applied as concentrated forces on nodes along web-compression flange junction. The Eigenvalue analysis is performed using 'LINEAR PERTURBATION' analysis option available in ABAQUS, and critical buckling load and deformed shapes corresponding to the first mode is evaluated. For comparing buckling loads using GBTUL, a numerical solution is considered, and analysis is performed by considering 20 GBT beam finite elements in the longitudinal direction, and cross-sectional discretization, material properties,

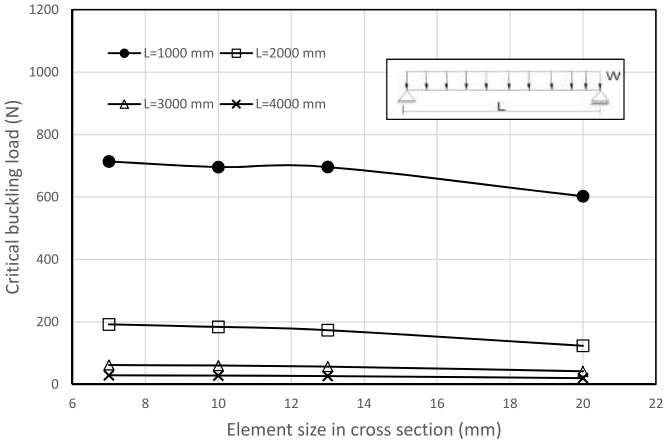

Fig. 5. Mesh sensitivity analysis in SFSM.

and end conditions are incorporated as same as that of SFSM and FEM. In the unconstrained buckling analysis, all the GBT modes are considered for calculating elastic buckling load, whereas in constrained buckling analysis, only specified modes are considered in GBTUL.

The comparison of critical buckling load for different member lengths corresponding to uniformly distributed load (UDL), uniformly varying load (UVL) and concentrated load (CONC) is shown in Figs. 6–8, respectively. For the span of beam less than 1000 mm, local buckling mode has been observed in the cross-section, and for lengths greater than 3000 mm, the beam buckles in the flexural torsional mode for all the loading cases. For intermediate lengths, the interaction of different modes is observed. For UDL and UVL, the SFSM results are comparable with FEM and GBT results. Minor variations exist in the buckling load prediction for spans between 1000 mm and 1600 mm determined using all the three methods, and this may be due to the differences in the points of modal change and nodal degrees of freedom considered in all the three analysis methods. For concentrated loading, variations up to 15% exist in the elastic buckling load prediction by SFSM for spans less than 1000 mm. Such short beams are seldom used in practice. However, for spans greater than 1000 mm, a reasonable comparison is achieved for predictions by all the three methods.

Fig. 9 shows the buckled mode shapes of beams for spans 500 mm and 1000 mm determined from buckling analysis in SFSM and FEM for UDL with simply supported end condition. It may be noted that the beams are plotted not to scale, and the buckling modes are amplified for clarity in deformed mode shape. It is evident that the fundamental mode shape is identical while comparing both the methods, and localized buckling is observed at regions of maximum flexural stress along the length of the beam.

4.2. Mode decomposition for different loads

Constrained buckling analysis is performed using SFSM on flexural member with lipped channel cross-section shown in Fig. 2 to decompose the buckling load in SFSM into pure local (L), distortional (D) and global (G) buckling loads for UDL, UVL, and CONC loading conditions. Since decomposition of buckling modes is not directly possible in FEM using ABAQUS, the comparison of pure buckling mode evaluated used SFSM is performed with GBTUL by considering local, distortional and global buckling modes separately for different spans of the member. The beam is divided into 20 sections along the length of the beam to incorporate local spline functions, and hence the restraint matrices in SFSM are evaluated by considering all the 20 possible half buckling waves along the longitudinal direction of the beam.

The comparison of SFSM and GBT results for pure buckling loads corresponding to global, distortional, and local buckling for different member lengths are presented in Figs. 10–12 respectively for UDL, UVL,

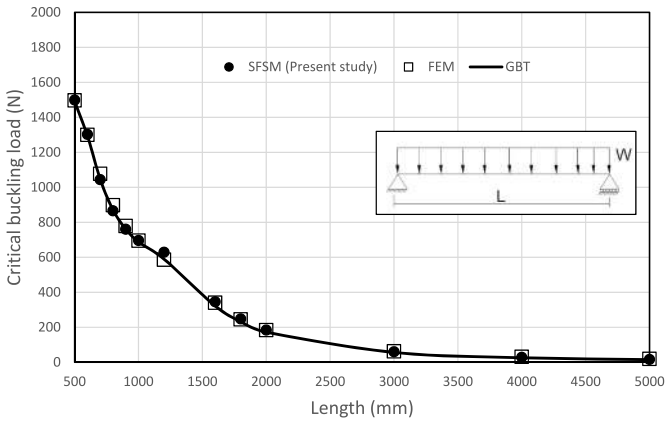

Fig. 6. Comparison of critical buckling load for uniformly distributed load (UDL).

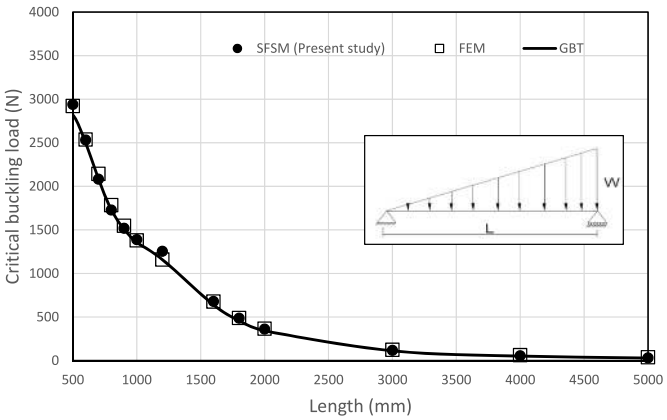

Fig. 7. Comparison of critical buckling load for uniformly varying load (UVL).

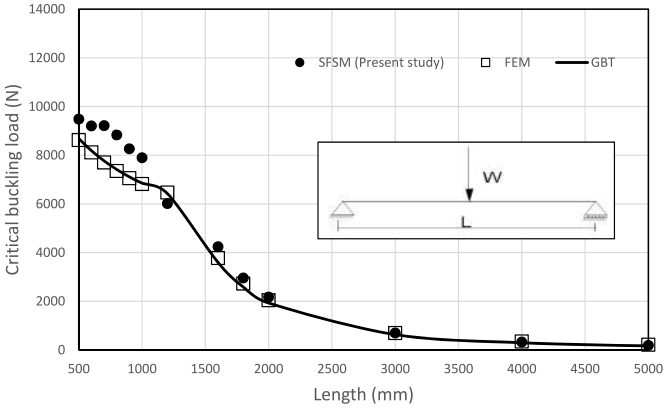

Fig. 8. Comparison of critical buckling load for concentrated load (CONC).

and CONC loading conditions. Though SFSM is not able to exactly replicate GBT results, there is a good agreement in pure buckling modes. The variations in local buckling load prediction are due to the differences in the pure local buckling assumption implemented in GBT and cSFSM, respectively. In GBT, pure buckling modes are determined directly from GBT fundamental equations, whereas in cFSM and cSFSM, the restraint matrix corresponding to local buckling mode is determined from a set of mechanical assumptions [20]. Also, for the discretization of cross-section incorporated in the present study, GBT produces 18 local buckling modes, whereas SFSM incorporates 36 base vectors for local mode in the restraint matrix corresponding to pure local buckling mode.

4.3. Calculation of mode participation in SFSM

From generalized buckling mode shape of flexural member determined using SFSM, the participation of local distortional, global, and shear/transverse extension modes are calculated, and percentage participation of different modes are compared with GBT results. Uniformly distributed load (UDL) with simply supported end condition is considered in the analysis for spans varying from 500 mm to 5000 mm. The load position and cross-sectional as well as longitudinal discretization is the same as that of mode decomposition study in section 4.2. For calculation of mode participation percentages, the restraint matrices are interpolated for section knots along the length of the beam by considering the participation of all the 20 half buckling waves along the length of the beam.

Fig. 13 represents the mode participation percentages corresponding to UDL for different member lengths determined using SFSM and GBT. It has to be noted that only local (L) or global (G) buckling modes are predominant for all the member lengths corresponding to the selected

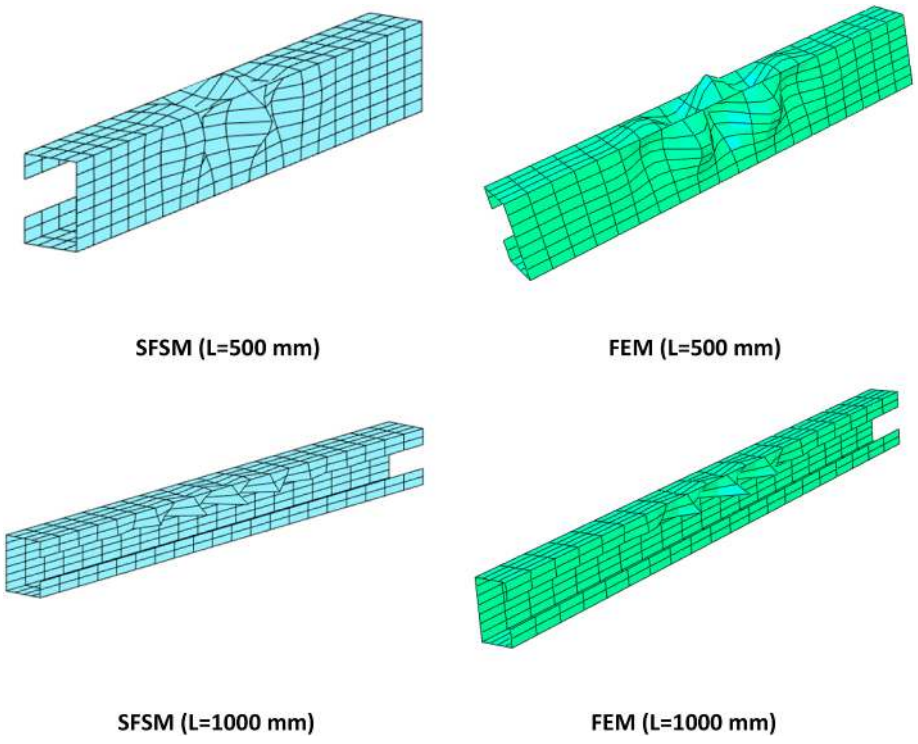

Fig. 9. Buckled modes of beams.

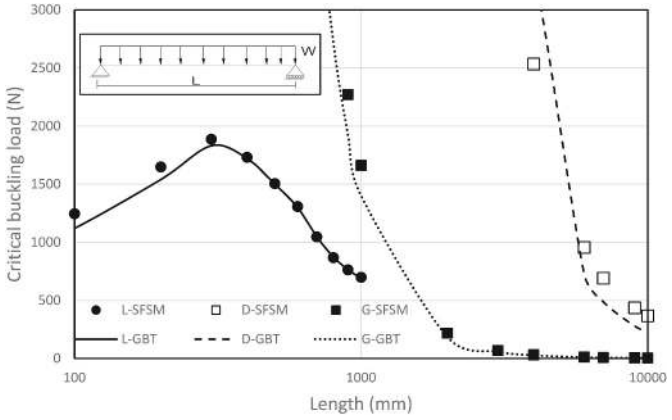

Fig. 10. Decomposition of buckling modes for uniformly distributed load (UDL).

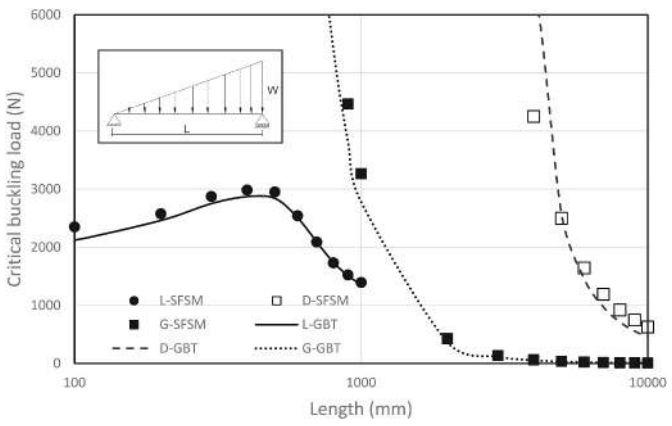

Fig. 11. Decomposition of buckling modes for uniformly varying load (UVL).

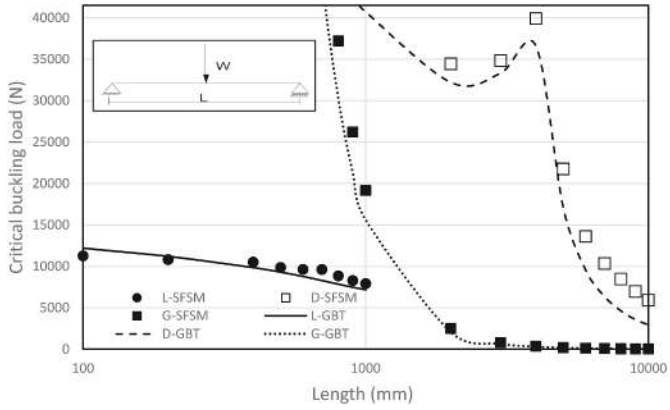

Fig. 12. Decomposition of buckling modes for concentrated load (CONC).

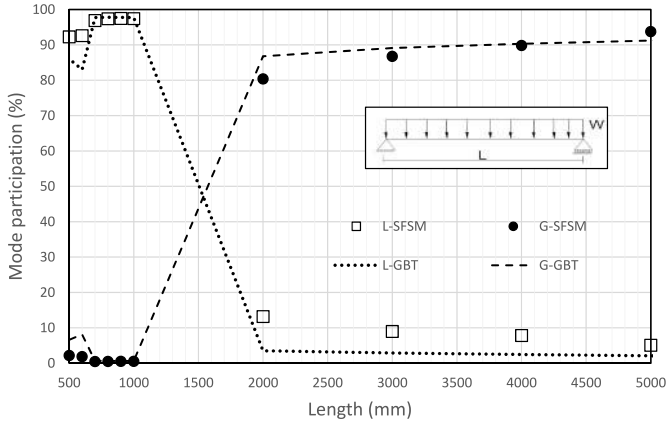

Fig. 13. Identification of buckling modes for UDL.

cross-section dimensions. The participation percentages of distortional (D) and shear/transverse extension (S/T) basis vectors are less than 10% for all the member lengths compared in the analysis. For spans less than 700 mm, the contribution of local buckling modes determined using GBT is lesser compared to SFSM, and the global buckling contribution calculated using GBT is nearly 10%. However, SFSM predicts local buckling participation percentage greater than 90% and global buckling contribution less than 3% as per engineering expectation for spans less than 700 mm. For beam spans greater than 700 mm, the mode participations for local and global buckling determined using SFSM and GBT are comparable. The variations in the participation of local and global modes determined using SFSM and GBT are due to the differences in basic assumption for local buckling mode, as highlighted in section 4.2. It is evident that the higher participation of local mode in SFSM for a span greater than 2000 mm is due to consideration of a greater number of base vectors corresponding to local mode than GBT. In all these examples, a lower limit of beam length of 500 mm is considered, because beams of this size and less are rarely used in practice.

4.4. Incorporation of intermediate restraints and other support conditions

Intermediate restraints, as well as different end supports, are incorporated in flexural members subjected to transverse load to calculate elastic buckling load using SFSM. The example problems shown in Fig. 14 includes three different conditions; (a) beam subjected to uniformly distributed load (UDL) having one end with fixed support and other end having roller support, (b) simply supported beam subjected to UDL in the presence of discrete intermediate lateral restraints (3 restraints) at web-compression flange junction and (c) simply supported beam with uniformly varying loading (UVL) and continuous lateral restraints (on all load points). Lipped channel cross-section with dimensions, discretization, and loading details depicted in Fig. 2 has been used for this study. The lateral constraints are imposed at intermediate locations by arresting the global degree of freedom in X direction using the Lagrange multiplier technique. Different end conditions are incorporated in SFSM by amendment of cubic end splines in the formulation. The modified elastic and geometric stiffness matrix developed after imposing constraints are utilized for unconstrained buckling analysis and mode decomposition.

Unconstrained buckling analysis is performed for the three example problems using SFSM and the critical buckling load evaluated are compared using FEM for spans varying from 500 mm to 5000 mm as in Figs. 15–17. For all the support conditions considered, the beam buckles in local mode for span less than 1000 mm. For larger spans (greater than 3000 mm), global buckling mode is observed, and for intermediate lengths, interactive buckling mode is visible. The presence of lateral supports arrest the lateral deformation in the case of intermediate and continuous lateral supports, and the global mode is governed by torsion rather than lateral displacement in those cases. For beam having fixed and roller end supports, a close comparison of critical elastic buckling load has been observed. When intermediate restraints are imposed in the beam, variations exist in the calculations by SFSM and FEM for

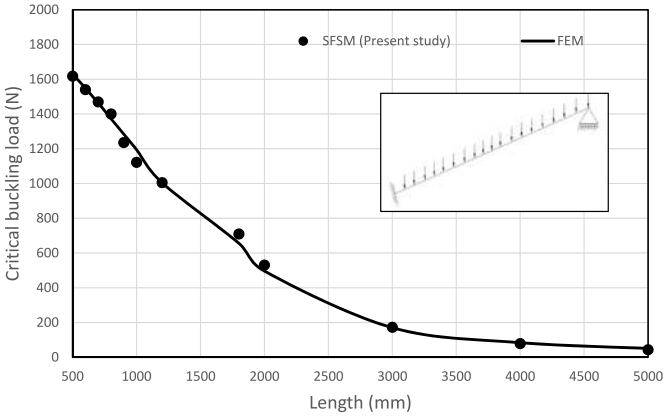

Fig. 15. Unconstrained buckling analysis for UDL with fixed and roller end supports.

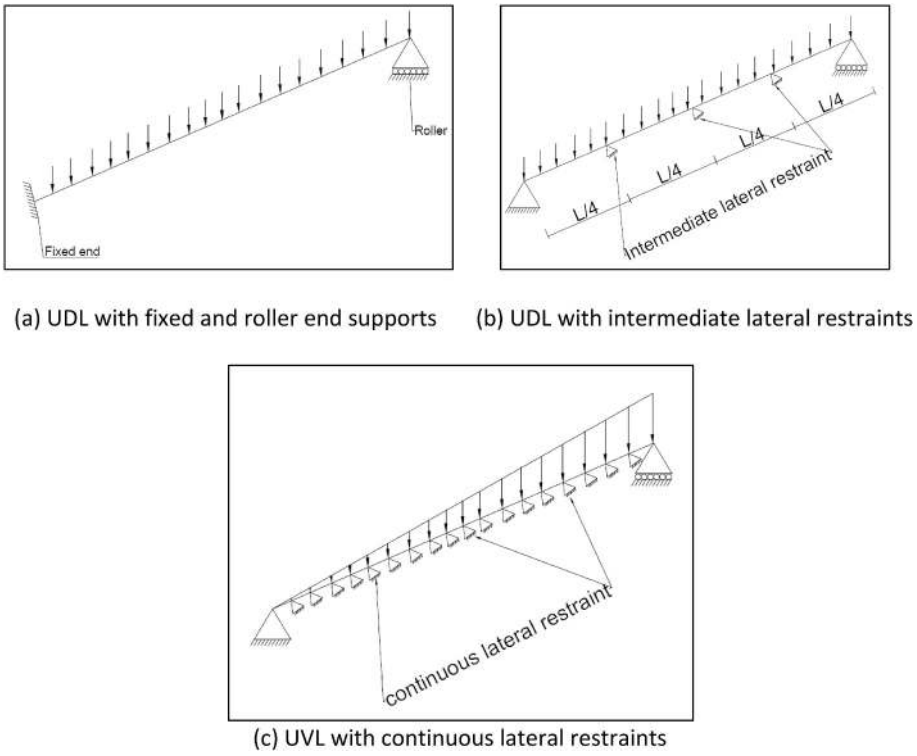

Fig. 14. Incorporation of intermediate restraints and different end conditions.

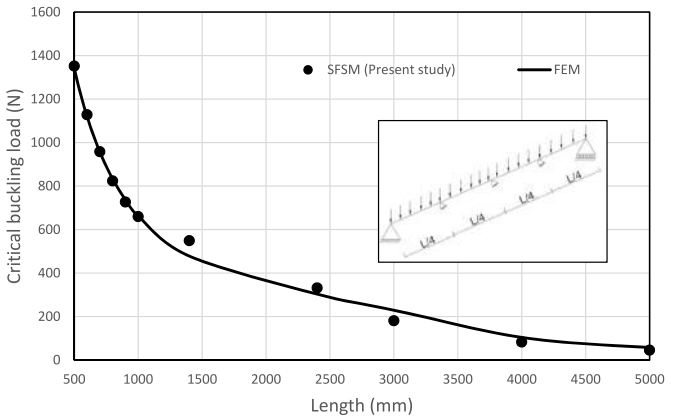

Fig. 16. Unconstrained buckling analysis for UDL with intermediate lateral restraints.

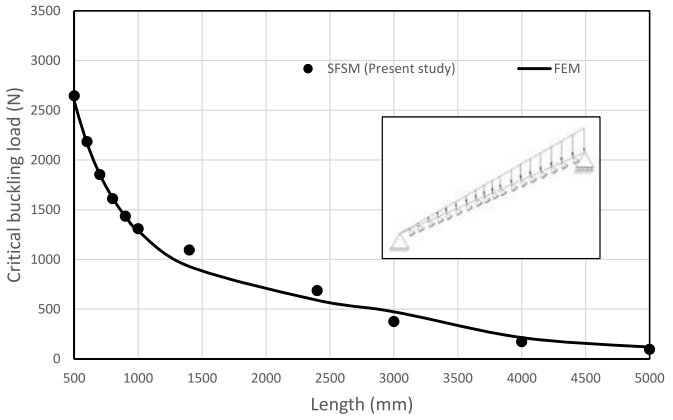

Fig. 17. Unconstrained buckling analysis for UVL with continuous lateral restraints.

intermediate spans (between 1000 mm and 3000 mm). However, these variations are less than 10%, and the possible reason can be the differences in the nodal degree of freedom incorporated in SFSM and FEM.

The decomposition of buckling modes for calculating pure elastic buckling loads for spans varying from 100 mm to 10000 mm using SFSM for different supports and intermediate restraints are shown in Figs. 18–20, and the calculated buckling loads are compared with GBT results. It is evident that for the cross-section incorporated in this study, the percentage contribution of local or global mode is more than 85% for all the spans considered (Fig. 13). Since distortional mode is a cross-sectional buckling mode, the same trend has been observed for examples present in this section and hence omitted in the present comparison. The trend observed in the calculation of pure elastic buckling load for global and local buckling is comparable in all the three examples highlighted in this section. The variations in local buckling loads are due to the difference in the mechanical assumption incorporated in GBT and cSFSM for the calculation of local mode, as highlighted in section 4.2.

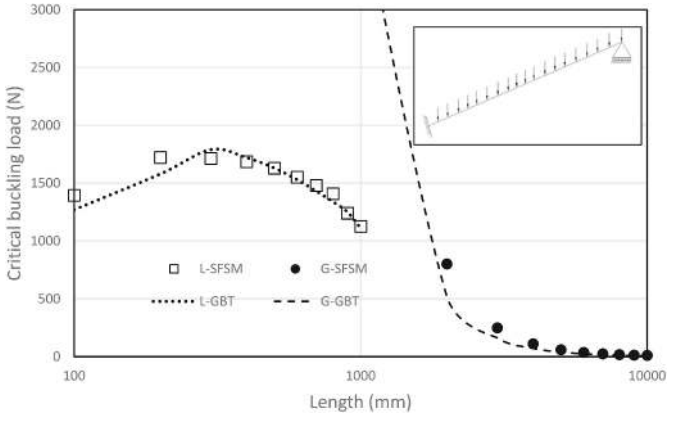

Fig. 18. Mode decomposition for UDL with fixed and roller end supports.

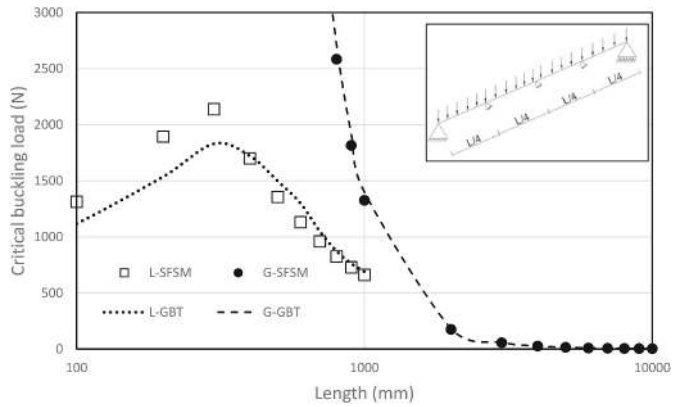

Fig. 19. Mode decomposition for UDL with intermediate lateral restraints.

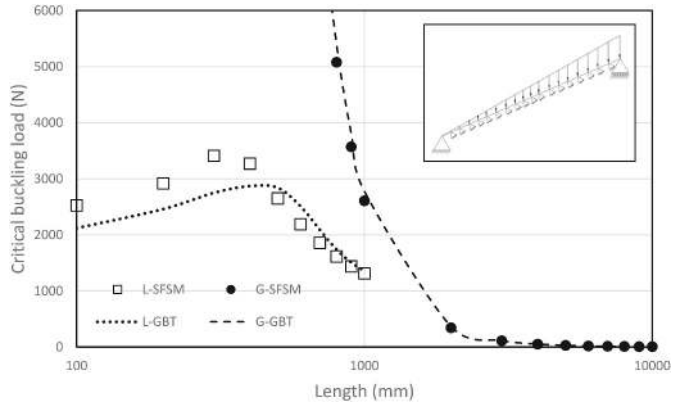

Fig. 20. Mode decomposition for UVL with continuous lateral restraints.

4.5. *Influence of moment gradient on pure buckling stresses*

Since the present study deals with flexural stress variation along the length of the thin-walled flexural member, it is important to highlight the influence of moment gradient on pure buckling modes. A plot of pure elastic buckling stresses for a beam having simply supported ends with

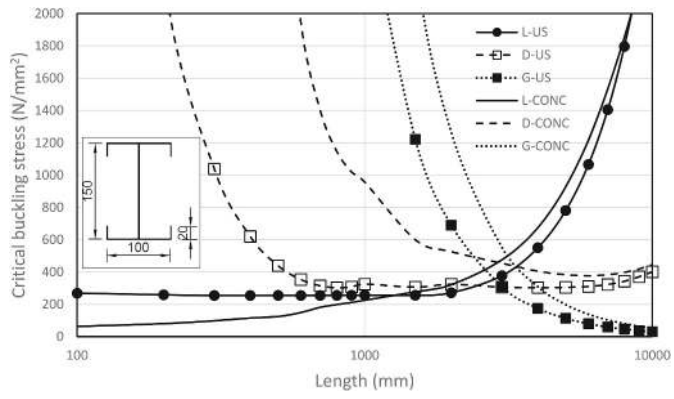

Fig. 21. Influence of moment gradient on pure buckling stresses.

variation of the span is presented in Fig. 21 on lipped I beam by applying uniform flexural stress (US) along the length of the member. The results are compared with maximum flexural stress due to concentrated force (CONC) applied at the centroid of the cross-section at mid-span, which provides a triangular variation of flexural stress along the length of the member. The lipped I section has been chosen to avoid torsion on the member, since the load passes through the shear center of cross-section. The cross-section is discretized by considering three intermediate nodes in the web, two in flanges and one in lips respectively, and the thickness of cross-section is adopted as 1 mm.

The moment gradient imposed in the member due to concentrated force provides a definite advantage in terms of pure distortional and global buckling stresses. For spans between 1000 mm and 10000 mm, the pure buckling stresses increase for distortional and global buckling with a maximum variation of 95% and 75% respectively for a range of spans. However, the increase in buckling stress due to moment gradient on local buckling stress is marginal (less than 20%) for a certain range of spans. Also, it is interesting to note the reduction in local buckling stress for spans less than 1000 mm due to high shear stress arising in the plate in addition to longitudinal flexural stress.

5. Conclusion

Though mode decomposition studies in the context of SFSM are reported in the literature, the added advantages of cSFSM over cFSM in incorporating longitudinal variations of stresses and intermediate restraints for mode decomposition and mode identification is the novelty of the present formulation. For incorporating longitudinal stress variation for beams subjected to general transverse loading, the membrane stresses are evaluated by performing static analysis of beam subjected to transverse loads. The deflection corresponding to transverse loads is calculated, and the membrane stresses corresponding to different plate strips are calculated and imposed in the geometric stiffness matrix corresponding to the membrane and flexural degree of freedom. The modified geometric stiffness matrix is incorporated for calculating elastic buckling loads, pure buckling loads, and mode participation percentages. The intermediate restraints to the degree of freedom are incorporated using Lagrange multiplier technique in static and Eigenvalue analysis, and different support conditions are imposed by amendment of cubic end splines.

Example problems are presented for different spans corresponding to unconstrained buckling analysis, mode decomposition, mode identification, and analysis in the presence of intermediate restraints and different supports. The elastic buckling loads determined using SFSM are comparable with FEM and GBT results for most of the practical spans for the thin-walled flexural member. Mode decomposition and mode identification results determined using cSFSM follow the same trend as in GBT, even though the analysis procedures in both these methods are not identical. The developed formulation is useful for determining elastic buckling stresses for local, distortional, and global buckling and calculation of mode participation percentages in the context of the design of thin-walled steel members using DSM for flexural members subjected to general transverse loads.

Authorship contribution statement

S S Ajeesh: Conceptualization, Methodology, Investigation, Writing Original draft. **S Arul Jayachandran**: Conceptualization, Methodology, Supervision, Writing-review and editing.

Declaration of competing interest

The authors declare that they have no known competing financial interests or personal relationships that could have appeared to influence the work reported in this paper.

References

[1] Y.K. Cheung, Finite strip method analysis of elastic slabs, J. Eng. Mech. Div. ASCE. 94 (1968) 1365–1378.

[2] G.J. Hancock, Local, distortional and lateral buckling of I- beams, J. Struct. Div. ASCE 104 (1978) 1787–1798.

[3] H.C. Bui, Buckling analysis of thin-walled sections under general loading conditions, Thin-Walled Struct. 47 (2009) 730–739, https://doi.org/10.1016/j.tws.2008.12.003.

[4] G.J. Hancock, C.H. Pham, Buckling analysis of thin-walled sections under localised loading using the semi-analytical finite strip method, Thin-Walled Struct. 86 (2015) 35–46, https://doi.org/10.1016/j.tws.2014.09.017.

[5] X.T. Chu, Z.M. Ye, R. Kettle, L.Y. Li, Buckling behaviour of cold-formed channel sections under uniformly distributed loads, Thin-Walled Struct. 43 (2005) 531–542, https://doi.org/10.1016/j.tws.2004.10.002.

[6] V.V. Nguyen, G.J. Hancock, C.H. Pham, Analyses of thin-walled sections under localised loading for general end boundary conditions – Part 2 : Buckling, Thin-Walled Struct. 119 (2017) 973–987, https://doi.org/10.1016/j.tws.2017.01.008.

[7] R. Schardt, Generalized beam theory an adequate method for coupled stability problems, Thin-Walled Struct. 19 (1994) 161–180.

[8] D. Camotim, N. Silvestre, C. Basaglia, R. Bebiano, GBT-based buckling analysis of thin-walled members with non-standard support conditions, Thin-Walled Struct. 46 (2008) 800–815, https://doi.org/10.1016/j.tws.2008.01.019.

[9] S.C. Fan, Spline Finite Strip in Structural Analysis (PhD Thesis), The University of Hongkong, 1982.

[10] S.C.W. Lau, G.J. Hancock, Buckling of thin flat-walled structures by a spline finite strip method, Thin-Walled Struct. 4 (1986) 269–294, https://doi.org/10.1016/0263-8231(86)90034-0.

[11] S.C.W. Lau, G.J. Hancock, Inelastic buckling analyses of beams, columns and plates using the spline finite strip method, Thin-Walled Struct. 7 (1989) 213–238, https://doi.org/10.1016/0263-8231(89)90026-8.

[12] G.J. Hancock, A.J. Davids, P.W. Key, S.C.W. Lau, K.J.R. Rasmussen, Recent developments in the buckling and nonlinear analysis of thin-walled structural members, Thin-Walled Struct. 9 (1990) 309–338, https://doi.org/10.1016/0263-8231(90)90050-9.

[13] Y.B. Kwon, G.J. Hancock, A nonlinear elastic spline finite strip analysis for thin-walled sections, Thin-Walled Struct. 12 (1991) 295–319, https://doi.org/10.1016/0263-8231(91)90031-D.

[14] G. Eccher, K.J.R. Rasmussen, R. Zandonini, Elastic buckling analysis of perforated thin-walled structures by the isoparametric spline finite strip method, Thin-Walled Struct. 46 (2008) 165–191, https://doi.org/10.1016/j.tws.2007.08.030.

[15] G. Eccher, K.J.R. Rasmussen, R. Zandonini, Geometric nonlinear isoparametric spline finite strip analysis of perforated thin-walled structures, Thin-Walled Struct. 47 (2009) 219–232, https://doi.org/10.1016/j.tws.2008.05.013.

[16] Z. Yao, K.J.R. Rasmussen, Material and geometric nonlinear isoparametric spline finite strip analysis of perforated thin-walled steel structures—analytical developments, Thin-Walled Struct. 49 (2011) 1359–1373, https://doi.org/10.1016/j.tws.2011.06.004.

[17] Z. Yao, K.J.R. Rasmussen, Material and geometric nonlinear isoparametric spline finite strip analysis of perforated thin-walled steel structures - numerical investigations, Thin-Walled Struct. 49 (2011) 1374–1391, https://doi.org/10.1016/j.tws.2011.06.005.

[18] S. Ádány, B.W. Schafer, Buckling mode decomposition of single-branched open cross-section members via finite strip method: Derivation, Thin-Walled Struct. 44 (2006) 563–584, https://doi.org/10.1016/j.tws.2006.03.013.

[19] S. Ádány, B.W. Schafer, Buckling mode decomposition of single-branched open cross-section members via finite strip method: application and examples, Thin-Walled Struct. 44 (2006) 585–600, https://doi.org/10.1016/j.tws.2006.03.014.

[20] S. Ádány, B.W. Schafer, A full modal decomposition of thin-walled, single-branched open cross-section members via the constrained finite strip method, J. Constr. Steel Res. 64 (2008) 12–29, https://doi.org/10.1016/j.jcsr.2007.04.004.

[21] N. Djafour, M. Djafour, A. Megnounif, M. Matallah, D. Zendagui, A constrained finite strip method for prismatic members with branches and/or closed parts, Thin-Walled Struct. 61 (2012) 42–48, https://doi.org/10.1016/j.tws.2012.04.020.

[22] S. Ádány, B.W. Schafer, Generalized constrained finite strip method for thin-walled members with arbitrary cross-section: primary modes, Thin-Walled Struct. 84 (2014) 150–169, https://doi.org/10.1016/j.tws.2014.06.001.

[23] S. Ádány, B.W. Schafer, Generalized constrained finite strip method for thin-walled members with arbitrary cross-section: secondary modes, orthogonality, examples, Thin-Walled Struct. 84 (2014) 123–133, https://doi.org/10.1016/j.tws.2014.06.002.

[24] Z. Li, B.W. Schafer, Constrained finite strip method for thin-walled members with general end boundary conditions, J. Eng. Mech. 139 (2013) 1566–1576, https://doi.org/10.1061/(ASCE)EM.1943-7889.0000591.

[25] Z. Li, M.T. Hanna, S. Ádány, B.W. Schafer, Impact of basis, orthogonalization, and normalization on the constrained Finite Strip Method for stability solutions of open thin-walled members, Thin-Walled Struct. 49 (2011) 1108–1122, https://doi.org/10.1016/j.tws.2011.04.003.

[26] M. Casafont, F. Marimon, M.M. Pastor, Calculation of pure distortional elastic buckling loads of members subjected to compression via the finite element method, Thin-Walled Struct. 47 (2009) 701–729, https://doi.org/10.1016/j.tws.2008.12.001.

[27] M. Casafont, F. Marimon, M. Pastor, M. Ferrer, Linear buckling analysis of thin-walled members combining the generalised beam theory and the finite element method, Comput. Struct. 89 (2011) 1982–2000, https://doi.org/10.1016/j.compstruc.2011.05.016.

[28] A.L. Joó, S. Ádány, FEM-based approach for the stability design of thin-walled members by using cFSM base functions, Period. Polytech. Civ. Eng. 53 (2009) 61–74, https://doi.org/10.3311/pp.ci.2009-2.02.
[29] S. Ádány, A.L. Joó, B.W. Schafer, Buckling mode identification of thin-walled members by using cFSM base functions, Thin-Walled Struct. 48 (2010) 806–817, https://doi.org/10.1016/j.tws.2010.04.014.
[30] M. Nedelcu, GBT formulation to analyse the behaviour of thin-walled members with variable cross-section, Thin-Walled Struct. 48 (2010) 629–638, https://doi.org/10.1016/j.tws.2010.03.001.
[31] Z. Li, S. Ádány, B.W. Schafer, Modal identification for shell finite element models of thin-walled members in nonlinear collapse analysis, Thin-Walled Struct. 67 (2013) 15–24, https://doi.org/10.1016/j.tws.2013.01.019.
[32] S. Ádány, Shell element for constrained finite element analysis of thin-walled structural members, Thin-Walled Struct. 105 (2016) 135–146, https://doi.org/10.1016/j.tws.2016.04.012.
[33] S. Ádány, Constrained shell Finite Element Method for thin-walled members, Part 1: constraints for a single band of finite elements, Thin-Walled Struct. (2017), https://doi.org/10.1016/j.tws.2017.01.015.
[34] S. Ádány, D. Visy, R. Nagy, Constrained shell Finite Element Method, Part 2: application to linear buckling analysis of thin-walled members, Thin-Walled Struct. (2017), https://doi.org/10.1016/j.tws.2017.01.022.
[35] S. Ádány, Constrained shell finite element method for thin-walled members with holes, Thin-Walled Struct. 121 (2017) 41–56, https://doi.org/10.1016/j.tws.2017.09.021.
[36] M. Khezri, K.J.R. Rasmussen, An energy-based approach to buckling modal decomposition of thin-walled members with arbitrary cross sections , Part 1 : Derivation, Thin-Walled Struct. 138 (2019) 496–517, https://doi.org/10.1016/j.tws.2019.01.041.
[37] M. Khezri, K.J.R. Rasmussen, An energy-based approach to buckling modal decomposition of thin-walled members with arbitrary cross-sections , Part 2 : modified global torsion modes , examples, Thin-Walled Struct. 138 (2019) 518–531, https://doi.org/10.1016/j.tws.2019.01.043.
[38] S.S. Ajeesh, S. Arul Jayachandran, A constrained spline finite strip method for the mode decomposition of cold-formed steel sections using GBT principles, Thin-Walled Struct. 113 (2017) 83–93, https://doi.org/10.1016/j.tws.2017.01.004.
[39] S.S. Ajeesh, S. Arul Jayachandran, Identification of buckling modes in generalized spline finite strip analysis of cold-formed steel members, Thin-Walled Struct. 119 (2017) 593–602, https://doi.org/10.1016/j.tws.2017.07.005.
[40] M. Djelil, N. Djafour, M. Matallah, M. Djafour, Constrained spline Finite Strip Method for thin-walled members with open and closed cross-sections, Thin-Walled Struct. 132 (2018) 302–315, https://doi.org/10.1016/j.tws.2018.07.052.
[41] SIMULIA, Abaqus Analysis User's Manual, 2014.
[42] Generalized Beam Theory Research Group at Lisbon, Instituto Superior Técnico, University of Lisbon, Portugal, 2015. http://www.civil.ist.utl.pt/gbt/.